

Nickel(II) and Cobalt(II) 3-Hydroxy-4-pyridinone Complexes: Synthesis, Characterization and Speciation Studies in Aqueous Solution

Carla Queiros,^[a] M. João Amorim,^[b] Andreia Leite,^[b] Monica Ferreira,^[b] Paula Gameiro,^[b] Baltazar de Castro,^[b] Krzysztof Biernacki,^[b] Alexandre Magalhães,^[b] John Burgess,^[c] and Maria Rangel^{*[a]}

Keywords: Nickel / Cobalt / Toxicology / Pollution / N ligands / Ligand effects

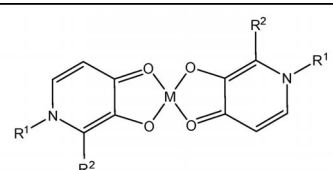
The interaction of nickel(II) and cobalt(II) with a set of 3-hydroxy-4-pyridinone ligands (Hmpp, Hmepp, Hetpp, Hempp, Hdepp and Hdmp) was investigated in aqueous solution. The family of chelators under study is pharmaceutically relevant in the treatment of iron-overloaded patients and it is foreseen to be of use in occupational health situations associated with accumulation of nickel and cobalt such as nasal/pulmonary and skin hazards and allergies. Ligand dissociation constants and stability constants for the cobalt(II) and nickel(II) complexes have been determined by potentiometric methods allowing the establishment of the corresponding speciation plots as a function of pH. The values of the stability constants are consistent with the Irving–Williams series and indicate the formation of stable ML₂ complexes which were isolated and characterized. Following the trend observed for 3-hydroxy-4-pyridinone ligands the solids were obtained as hydrates whose composition was characterized as [ML₂(H₂O)₂] \cdot xH₂O complexes. DFT calculations allowed geometry optimization and provided information about bond lengths and angles.

The interaction of nickel(II) and cobalt(II) with a set of 3-hydroxy-4-pyridinone ligands (Hmpp, Hmepp, Hetpp, Hempp, Hdepp and Hdmp) was investigated in aqueous solution. The family of chelators under study is pharmaceutically relevant in the treatment of iron-overloaded patients and it is foreseen to be of use in occupational health situations associated with accumulation of nickel and cobalt such as nasal/pulmonary and skin hazards and allergies. Ligand dissociation constants and stability constants for the cobalt(II) and nickel(II) complexes have been determined by potentiometric methods allowing the establishment of the corresponding speciation plots as a function of pH. The values of the stability constants are consistent with the Irving–Williams series and indicate the formation of stable ML₂ complexes which were isolated and characterized. Following the trend observed for 3-hydroxy-4-pyridinone ligands the solids were obtained as hydrates whose composition was characterized as [ML₂(H₂O)₂] \cdot xH₂O complexes. DFT calculations allowed geometry optimization and provided information about bond lengths and angles.

Introduction

3-Hydroxy-4-pyridinones (3,4-HPO's) are a family of ligands that can be prepared from 3-hydroxy-4-pyranones, naturally occurring compounds. Both classes of ligands and respective complexes have been extensively studied due to their broad field of application namely in therapeutics and diagnosis, solvent extraction and chemical analysis.^[1–6] 3-Hydroxy-4-pyridinones are heterocyclic compounds that include a nitrogen atom in the ring and hydroxylic and ketonic oxygen atoms in positions 3 and 4, respectively (Figure 1) which confer the strong chelating properties exhibited by the ligands towards M^{II}/M^{III} metal ions. The ligands are synthetically versatile allowing the introduction of different substituents in several positions of the heterocyclic ring without producing a significant change in complexation ability and acid–base properties.^[7–10] This characteristic is very important since changes in ligand lipophilicity are straightforwardly achieved generating ligands that are able to partition between aqueous and organic phases, namely in liposomes and biological membranes. In ad-

dition, 3-hydroxy-4-pyridinone ligands have other important characteristics, like predominance of the zwitterionic form at neutral pH, that promote their selection as chelating units for the design of ligands with pharmaceutical potential. The compound 3-hydroxy-1,2-dimethyl-4-pyridinone, commercially known as Deferiprone (DFP), has been extensively used as a therapeutical alternative to treat diseases associated with iron overload.^[11,12]



Complex	R ¹	R ²
M(mpp) ₂	H	CH ₃
M(etpp) ₂	H	CH ₂ CH ₃
M(dmpp) ₂	CH ₃	CH ₃
M(mepp) ₂	CH ₂ -CH ₃	CH ₃
M(empp) ₂	CH ₃	CH ₂ CH ₃
M(depp) ₂	CH ₂ -CH ₃	CH ₂ CH ₃

Figure 1. Formulae and abbreviations of the 3-hydroxy-4-pyridinone cobalt(II) and nickel(II) complexes studied in this work.

Ligands with the above chemical properties have an enormous potential as sequesters of metal ions, ensuring a protective measure against metal poisoning.^[13] Although many transition metals are known to be required for normal biological functions in humans it is also recognized that

[a] REQUIMTE, Instituto de Ciências Biomédicas de Abel Salazar, Universidade do Porto, 4099-003 Porto, Portugal
E-mail: mcrangel@fc.up.pt

[b] REQUIMTE, Departamento de Química e Bioquímica, Faculdade de Ciências, Universidade do Porto, 4099-003 Porto, Portugal

[c] Department of Chemistry, University of Leicester, Leicester, LE1 7RH, United Kingdom

Supporting information for this article is available on the WWW under <http://dx.doi.org/10.1002/ejic.201000849>.

the accumulation of metal ions in the body can produce more or less deleterious effects. For example, cobalt, the essential element of the B₁₂ system enzymes, is commonly used in materials like pigments and alloys and may lead to allergic dermatitis or asthma through industrial exposures although the occurrence of acute intoxications is rare.^[14,15] Nickel is more widely distributed being present in alloys and nickel-plated items, and the occupational exposure to it can cause nasal/pulmonary carcinogenic hazard and allergies like dermatitis.^[14,16]

In recent years chelation has been the most investigated way of removing toxic metal ions from the human body, and has also been of use to inhibit the active site of some metalloproteins.^[17]

In the context of an interest in the design of metal ion chelators and metal-based drugs, our group has long been interested in the chemistry of 3-hydroxy-4-pyridinones and their complexes.^[1,2,7] In the present work we paid particular attention to the interaction of a set of 3,4-HPO ligands of variable lipophilicity (Figure 1) with nickel(II) and cobalt(II) with the objective of determining their stability constants and establishment of speciation diagrams as a function of pH. This information, together with the characterization of the isolated metal chelates, is relevant for the possible use of 3,4-HPO ligands in the control of cobalt and nickel poisoning.

Results and Discussion

Synthesis and Characterization of Ligands

The synthesis of 3-hydroxy-4-pyridinones may be achieved by reaction of the appropriate 3-hydroxy-4-pyranone and an amine either by direct reaction or using the protection method in which the hydrogen atom of the enolic group is replaced by a benzyl group. From our experience and literature reports, it is known that the direct method works for small alkylamines but the protection method is preferred when amines with larger carbon chains are to be used. However, ligand synthesis by direct reaction presents difficulties in relation to purity and yield as the size of substituents increases; longer reaction times are necessary and the final products become oilier thus implying a less efficient extraction process. Considering the pK_a value of the OH group of 3-hydroxy-4-pyranones (pK_a between 8 and 9) and given that the initial pH of the reaction mixture is approximately 12 we tried a variant in which the hydroxy group is protected just by maintaining a lower pH (ca. 9) during the reaction course. The final product is extracted with dichloromethane yielding the 3-hydroxy-4-pyridinone in purer form. The method worked for the compounds reported here and the inconveniences of a larger number of steps, solvent consumption and final deprotection procedures have been avoided. Comparing the results obtained, it became clear that the variant with pH adjustment is a superior synthetic process, since the final compounds are purer, the yield is greater and the protection of the OH group with benzyl unnecessary. We recognize, however, that

the protection with the benzyl group must be used for more lipophilic compounds such as those derived from hexylamine. Ligands were characterized by mass spectrometry, FTIR, UV/Vis and ¹H NMR spectroscopy. Mass spectra show the expected peaks of the molecular ion M⁺ with values of m/z of 125, 153, 140, 153, 138/167 for Hmpp, Hmpep, Hetpp, Hempp and Hdepp, respectively. FTIR spectra exhibit typical bands around 3200, 1520/1460, 1630/1520 and 1250 cm⁻¹ associated with vibrations of the OH (aromatic), C=C (ring), C=O and C–O bonds. The values obtained are in agreement with those described in the literature.^[18,19] The UV/Vis spectra exhibit the expected bands assigned to the $\pi \rightarrow \pi^*$ electronic transitions, associated with the ethylene and benzenic linkages of the benzene ring usually observed at wavelengths between 210–280 nm. The ¹H NMR spectra obtained for the synthesized ligands generally exhibit a group of signals at 1/3 ppm corresponding to aliphatic protons and at 6/7.5 ppm (doublets) corresponding to aromatic protons. The OH group proton is not always observed but it originates a singlet at 8.8 ppm, while the N–H proton is a singlet that appears at δ = 11.4 ppm for Hmpp and Hetpp. A singlet is also observed for N–CH₃ (methyl group linked to nitrogen) at 3.8 ppm for Hempp.

Synthesis and Characterization of Complexes

The complexes were synthesized according to the method described by Gerard^[20] based on the reaction of the ligand with the metal ion nitrate in aqueous or aqueous/organic solution depending on the lipophilicity of the ligand. In order to avoid the concomitant formation of metal ion hydroxides a 1:2.2 metal-to-ligand ratio was used and ligand deprotonation was performed prior to solution mixture by raising the pH of the solution containing the ligand to 9.8. The reaction mixture was stirred for 12 h at room temperature. Water content of the isolated hydrates was quantified by the Karl Fischer method. The results obtained are consistent with those of elemental analysis thus confirming the number of water molecules associated with each complex. Hydration is generally observed in 3-hydroxy-4-pyridinone metal complexes as a consequence of the elevated tendency of the ligands to form hydrogen bonds.^[21]

Complexes were characterized by mass spectrometry, FTIR and UV/Vis spectroscopy; geometry optimization and information on bond lengths and angles was achieved by DFT calculations. Mass spectra obtained by electronic impact exhibited the peaks of the molecular ions [M]⁺, [M + H]⁺, [M + Na]⁺, [M + Na + H]⁺, and [M + Na + 2H]⁺ given in Table S1 (Supporting Information). FTIR spectra of the synthesized complexes present broad bands in the range from 3400–3500 cm⁻¹ assigned to the vibration of the OH group of the water molecules, narrow and low intensity bands in the region of 2830–3030 cm⁻¹ due to the C–H vibrations, stretching bands corresponding to C–C and C–O bonds between 1230–1290 cm⁻¹, and intense bands at 1870–1540 and 1550–1450 cm⁻¹ correspondent to vibrations of C=O and C=C of the aromatic ring. Bands in the region

from 450 to 690 cm^{-1} are also identified and are assigned to M–O bonds since they are not present in corresponding FTIR spectra of the ligands. In the case of complexes with mpp^- and etpp^- ligands the stretching bands corresponding to N–H and C–N bonds are generally masked by the vibration of the OH group or overlapping with C–C stretching, respectively.

The electronic spectra obtained in the visible region for the cobalt(II) and nickel(II) compounds are characteristic of high-spin d^7 and d^8 six-coordinate complexes with two types of ligands. Spectra are very similar for complexes of the same metal ion and for that reason we do not present here all spectra details but give the maximum wavelength for each complex in the Exp. Section. Illustrative examples relevant for the discussion are shown in Figure 2 for the complex $[\text{Co}(\text{empp})_2(\text{H}_2\text{O})_2]$ and in Figure 3 for the complex $[\text{Ni}(\text{dmpp})_2(\text{H}_2\text{O})_2]$, in each case dissolved in DMSO.

In the spectrum depicted in Figure 2 five bands are discernible at 457, 553, 597, 842 and 971 nm. Part of the characteristic lower energy band usually centred at ca. 1250 nm is also visible. This set of bands is generally attributed to

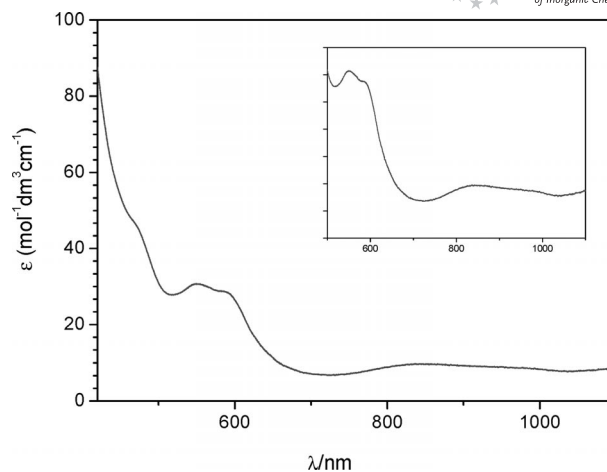


Figure 2. UV/Vis spectrum of $[\text{Co}(\text{empp})_2(\text{H}_2\text{O})_2]$ in DMSO.

high-spin d^7 cobalt(II) six-coordinated complexes in which two types of ligands are present. The bands at 457 nm ($\epsilon = 50 \text{ dm}^3 \text{ mol}^{-1} \text{ cm}^{-1}$) are assigned to spin-orbit effects or

Table 1. Most relevant geometrical parameters for cobalt(II) complexes, obtained at the B3LYP/6-31G(d,p) level.

	$[\text{Co}(\text{mpp})_2(\text{H}_2\text{O})_2]$	$[\text{Co}(\text{etpp})_2(\text{H}_2\text{O})_2]$	$[\text{Co}(\text{dmpp})_2(\text{H}_2\text{O})_2]$	$[\text{Co}(\text{mepp})_2(\text{H}_2\text{O})_2]$	$[\text{Co}(\text{depp})_2(\text{H}_2\text{O})_2]$	$[\text{Co}(\text{empp})_2(\text{H}_2\text{O})_2]$
Distance ^[a]						
O1–C1	1.280	1.283	1.283	1.282	1.282	1.282
C2–O2	1.309	1.310	1.311	1.313	1.314	1.313
(O2–C2)–(O1–C1)	0.029	0.027	0.028	0.031	0.032	0.031
C1–C2	1.465	1.461	1.460	1.461	1.459	1.460
C2–C3	1.390	1.390	1.393	1.392	1.392	1.392
C3–N	1.380	1.379	1.390	1.394	1.394	1.390
N–C4	1.354	1.355	1.358	1.357	1.358	1.359
C4–C5	1.374	1.375	1.375	1.375	1.375	1.374
C5–C1	1.420	1.420	1.415	1.414	1.415	1.417
Co–O1	2.060	2.053	2.052	2.063	2.065	2.067
Co–O2	2.077	2.056	2.053	2.045	2.045	2.042
Co–O3	2.237	2.281	2.280	2.277	2.280	2.279
Co–O3'	2.237	2.281	2.280	2.277	2.280	2.279
O1–H1	2.368	2.380	2.386	2.475	2.489	2.475
O2–H2	1.966	2.015	1.993	2.025	2.008	2.043
Angle ^[a]						
$\beta = \text{O1–Co–O1}'$	179.97	180.00	179.97	180.00	180.00	180.00
$\alpha = \text{O2–Co–O2}'$	180.00	179.97	179.97	180.00	180.00	197.97
$\tau = (\beta - \alpha)/60$	0.00	0.00	0.00	0.00	0.00	0.30
O3–Co–O3'	179.97	179.96	180.00	180.00	180.00	180.00
O1–Co–O2	80.10	80.75	80.56	81.03	81.14	81.15
O1–Co–O2'	99.90	99.25	99.44	98.97	98.86	98.85
O2–Co–O1'	99.90	99.25	99.44	98.97	98.86	98.85
O1–Co–O3	82.39	83.94	83.87	86.49	86.52	86.67
O2–Co–O3	77.29	78.07	77.80	78.43	78.21	78.68
O2'–Co–O3	102.71	101.93	102.20	101.54	101.79	101.32
Dihedral angle ^[a]						
O1–O2–O1'–O2'	0.00	0.00	0.00	0.00	0.00	0.00
O1–O3–O1'–O3'	0.00	0.00	0.00	0.00	0.00	0.00
O2–O3–O2'–O3'	0.00	0.00	0.00	0.00	0.00	0.00
O1–C1–C2–O2	0.95	0.29	0.93	0.48	0.02	0.01
C2–C1–O1–Co	12.91	14.62	14.49	14.96	14.47	15.04
C1–C2–O2–Co	14.00	14.90	15.73	15.77	14.65	15.21
C1–O1–Co–O3	93.85	96.18	96.11	96.75	86.52	96.80
C2–O2–Co–O3	100.39	102.87	103.52	106.26	105.22	105.97

[a] Distances in Å and angles in °. Numbering according to Figure 1.

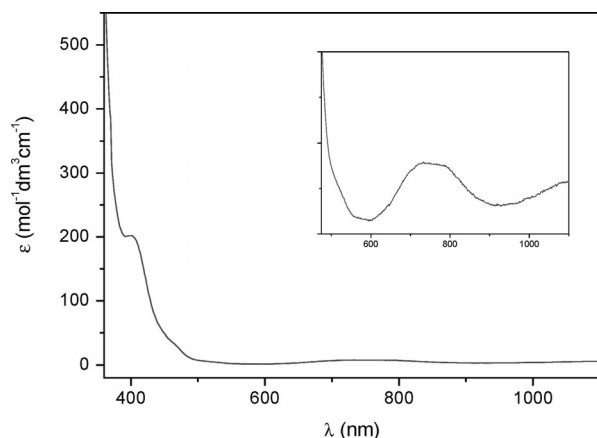


Figure 3. UV/Vis spectrum of $[\text{Ni}(\text{dmpp})_2(\text{H}_2\text{O})_2]$ in DMSO.

spin-forbidden transition to doublet states, the band at 597 nm ($\epsilon = 28 \text{ dm}^3 \text{ mol}^{-1} \text{ cm}^{-1}$) to the transition ${}^4\text{T}_1 \rightarrow {}^4\text{A}_2$, the band at 553 nm ($\epsilon = 31 \text{ dm}^3 \text{ mol}^{-1} \text{ cm}^{-1}$) to the transition ${}^4\text{T}$

$\rightarrow {}^4\text{T}_1$ (P) and the lower energy band ($>1100 \text{ nm}$) to the ${}^4\text{T}_1 \rightarrow {}^4\text{T}_2$ transition. The two bands at 842 and 971 nm ($\epsilon = 10 \text{ dm}^3 \text{ mol}^{-1} \text{ cm}^{-1}$), which in O_h symmetry coalesce into one, are also assigned to spin-orbit effects or spin-forbidden transition to doublet states.

The spectrum depicted in Figure 3 shows two bands at 399 and 750 nm and part of the characteristic lower energy band usually centred at ca. 1100 nm is also visible. Closer inspection allows distinction of the splitting of the band at 750 nm into two, a fact that is consistent with the presence of two ligands in the coordination sphere. This pattern of bands is generally observed for high-spin d^8 nickel(II) six-coordinated complexes with mixed ligands and is consistent with the green colour observed for the prepared complexes. The band at 399 nm ($\epsilon = 200 \text{ dm}^3 \text{ mol}^{-1} \text{ cm}^{-1}$) is assigned to the transition ${}^3\text{A}_2 \rightarrow {}^3\text{T}_1$ (P), the band at 748 nm ($\epsilon = 8 \text{ dm}^3 \text{ mol}^{-1} \text{ cm}^{-1}$) to the transition ${}^3\text{A}_2 \rightarrow {}^3\text{T}_1$ and the lower energy band (ca. 1100 nm) to the ${}^3\text{A}_2 \rightarrow {}^3\text{T}_2$ transition. A bathochromic shift of ca. 50 nm is observed when the solvent is changed from DMSO to methanol which suggests

Table 2. Most relevant geometrical parameters for nickel(II) complexes, obtained at the B3LYP/6-31G(d,p) level.

	$[\text{Ni}(\text{mpp})_2(\text{H}_2\text{O})_2]$	$[\text{Ni}(\text{etpp})_2(\text{H}_2\text{O})_2]$	$[\text{Ni}(\text{dmpp})_2(\text{H}_2\text{O})_2]$	$[\text{Ni}(\text{mepp})_2(\text{H}_2\text{O})_2]$	$[\text{Ni}(\text{depp})_2(\text{H}_2\text{O})_2]$	$[\text{Ni}(\text{empp})_2(\text{H}_2\text{O})_2]$
Distance ^[a]						
O1–C1	1.281	1.283	1.283	1.283	1.284	1.283
C2–O2	1.309	1.310	1.310	1.311	1.311	1.310
(O2–C2)–(O1–C1)	0.028	0.027	0.027	0.028	0.027	0.027
C1–C2	1.465	1.462	1.461	1.459	1.458	1.459
C2–C3	1.390	1.390	1.394	1.394	1.394	1.394
C3–N	1.381	1.379	1.390	1.393	1.393	1.390
N–C4	1.354	1.354	1.358	1.357	1.357	1.358
C4–C5	1.374	1.375	1.375	1.376	1.376	1.375
C5–C1	1.421	1.421	1.415	1.413	1.413	1.415
Ni–O1	2.033	2.033	2.032	2.032	2.033	2.033
Ni–O2	2.033	2.036	2.033	2.034	2.034	2.033
Ni–O3	2.170	2.172	2.174	2.176	2.177	2.175
Ni–O3'	2.170	2.172	2.174	2.176	2.177	2.175
O1–H1	2.384	2.367	2.353	2.338	2.318	2.327
O2–H2	1.995	2.005	1.995	1.990	2.001	2.010
Angle ^[a]						
$\beta = \text{O1–Ni–O1}'$	180.00	180.00	179.97	180.00	179.97	180.00
$\alpha = \text{O2–Ni–O2}'$	180.00	180.00	180.00	180.00	179.97	180.00
$\tau = (\beta - \alpha)/60$	0.00	0.00	0.00	0.00	0.00	0.00
O3–Ni–O3'	180.00	180.00	180.00	180.00	179.97	180.00
O1–Ni–O2	82.20	82.37	82.14	82.13	82.23	82.23
O1–Ni–O2'	97.80	97.63	97.86	97.87	97.78	97.77
O2–Ni–O1'	97.80	97.63	97.86	97.87	97.77	97.77
O1–Ni–O3	85.45	85.29	84.95	84.72	84.47	84.60
O2–Ni–O3	79.40	79.48	79.41	79.31	79.49	79.64
O2'–Ni–O3	100.59	100.52	100.59	100.69	100.51	100.36
Dihedral angle ^[a]						
O1–O2–O1'–O2'	0.01	0.00	0.00	0.00	0.00	0.00
O1–C1–C2–O2	0.76	0.13	0.75	0.73	0.18	0.14
O1–O3–O1'–O3'	0.00	0.00	0.00	0.00	0.00	0.00
O2–O3–O2'–O3'	0.01	0.00	0.00	0.00	0.00	0.00
C2–C1–O1–Ni	12.76	12.77	12.86	12.98	13.05	13.01
C1–C2–O2–Ni	13.75	12.84	13.86	13.94	13.25	13.15
C1–O1–Ni–O3	95.43	95.16	95.59	95.64	95.60	95.68
C2–O2–Ni–O3	102.5	101.57	102.16	102.04	101.22	101.24

[a] Distances in Å and angles in °. Numbering according to Figure 1.

that in solution the axial positions are occupied by solvent molecules.

In order to obtain structural information we performed DFT calculations to optimize geometry and obtain bond lengths and bond angles of complexes of the type $[M(L)_2(H_2O)_2]$ taking into account the stoichiometry of the isolated solids. The energy minimization of all the complexes was performed in gas phase at the B3LYP/6-31G(d,p) level without any type of symmetry constraints. The optimized values of the most relevant geometrical parameters for cobalt(II) and nickel(II) complexes are summarized in Tables 1 and 2, respectively.

All the structures correspond to a *trans* conformation of a tetragonal distorted metal ion coordination, as shown in Figure 4. The ligand oxygen atoms occupy equatorial positions and those of the two water molecules establish slightly longer coordination bonds about the axial positions. A few different geometries were also tested as starting points for energy minimization, namely the *cis* conformation where one of the ligands coordinates the central ion with one axial and one equatorial oxygen atom and the *cis* configurations of ligands. All these alternatives converged to the more stable geometries presented here.

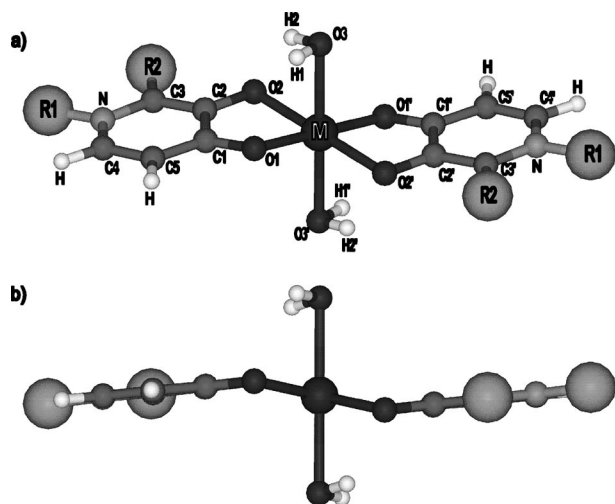


Figure 4. Typical optimized structure for *trans* conformation of cobalt(II) and nickel(II) complexes: a) perspective view; b) side view (R^1 and R^2 according to Figure 1).

Although the four equatorial oxygen atoms are coplanar, the planes of the pyridinone rings are parallel but not equidistant from the two water molecules (see part b of Figure 4); this is evident for instance by the different values of the angles $O2-M-O3$ and $O2'-M-O3$. The distances obtained predict that the two axial water molecules are able to establish hydrogen bond-type interactions with the equatorial oxygen atoms, the average distances $O1-H1$ and $O2-H2$ being 2.35 and 2.0 Å, respectively.

Comparing the structural data for complexes of the same metal ion it is evident that the different substituents in the pyridinone ring do not significantly change the structure of the complexes thus confirming the possibility of modifying the lipophilic character of ligands and complexes without

altering their coordination ability. On comparison of structural data for cobalt(II) and nickel(II) complexes of the same ligand the expected different metal–ligand distances are observed and according to the generated angle values it is possible to conclude that the geometry of the nickel(II) complexes is slightly less distorted in the equatorial plane than that of the cobalt(II) complexes.

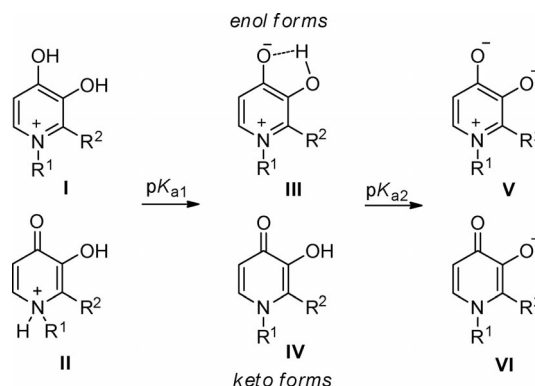
Acidity and Stability Constants

Since we were interested in determining stability constants for cobalt(II) and nickel(II) with the same set of 3,4-HPO and considering that the values reported in the literature for some of the ligands under study do not refer to the same experimental conditions we determined the protonation constants for the ligands used in this work. Acidity constants were determined from titration curves of stock solutions of the ligands prepared in the conditions described in the Exp. Section. Data were refined with the program Hyperquad^[22] and the values obtained are reported in Table 3.

Table 3. Acidity constants determined for the 3-hydroxy-4-pyridinones.

Ligand	pK_{a1}	pK_{a2}
Hmpp	3.62 ± 0.05	9.48 ± 0.05
Hetpp	3.63 ± 0.04	9.62 ± 0.05
Hdmpp	3.69 ± 0.01	9.61 ± 0.03
Hempp	3.53 ± 0.02	9.46 ± 0.05
Hmepp	3.53 ± 0.04	9.18 ± 0.04
Hdepp	3.49 ± 0.02	9.35 ± 0.06

The values of the acidity constants are similar for all the ligands thus meaning that tuning of the hydrophilic–lipophilic balance does not significantly change the acid–base properties. Moreover, the values of pK_{a1} (H_2L) are close to 3.5 and those of pK_{a2} (HL) close to 9.3, as has been observed in previous studies.^[8,23–25] As reported, for some of the ligands,^[1] the pK_{a1} values of the 3,4-HPO's are about 5 times greater than those of 3-hydroxy-4-pyrones due to the more efficient delocalization of the positive charge in the ring (Scheme 1). In relation to pK_{a2} the comparison of the obtained values for pyridinones (9.18–9.62),^[26] with those

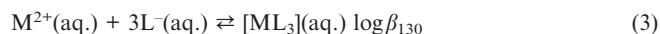
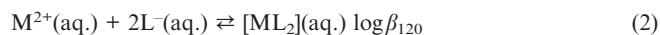
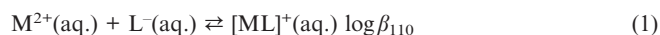


Scheme 1. Tautomeric equilibria for 3-hydroxy-4-pyridinones.

reported for maltol (8.44) and kojic acid (7.67),^[27] implies that pyridinone ligands are stronger bases.

The speciation diagrams generated with the values of dissociation constants are similar for all the 3,4-HPO ligands and provide evidence that the neutral species, HL, predominates in the pH range between 5 and 9 thus predicting a favourable absorption of the ligands by the body.^[28]

The values of the acidity constants of the ligands determined in this work, for metal ion protolysis and water protolysis, and those given in the literature that are valid under the experimental conditions of this work^[29] were used as fixed parameters in the refinement of data regarding the metal–ligand systems in accordance with the proposed model Equations (1), (2), (3), (4) and (5).



For the two metal ions and most of the ligands it was only possible to calculate the stability constants for the equilibria described by Equations (1) and (2).

The calculated stability constants for the set of 3-hydroxy-4-pyridinone ligands with cobalt(II) and nickel(II) are given in Tables 4 and 5, respectively. The stability constant values are indicative of a considerable affinity of the ligands towards cobalt(II) and nickel(II) and are very similar for both metal ions. The values of the stepwise stability constants are in agreement with the statistically expected values for this kind of complex for which no structural change is observed, i.e. $K_1 > K_2$.

Table 4. Stability constants determined for the 3-hydroxy-4-pyridinones/cobalt(II) complexes.

Ligand	Cobalt(II) systems		$\log k_2$
	$\log \beta_{110}$	$\log \beta_{120}$	
Hmpp	6.36 ± 0.04	11.13 ± 0.05	4.77 ± 0.06
Hetpp	6.22 ± 0.05	11.59 ± 0.05	5.37 ± 0.07
Hdmpp	6.66 ± 0.05	11.74 ± 0.04	5.08 ± 0.06
Hempp	6.01 ± 0.04	10.50 ± 0.05	4.49 ± 0.06
Hmepp	5.96 ± 0.04	10.11 ± 0.03	4.15 ± 0.05
Hdepp	6.10 ± 0.06	10.74 ± 0.06	4.64 ± 0.08

Table 5. Stability constants determined for the 3-hydroxy-4-pyridinones/nickel(II) complexes.

Ligand	Nickel(II) systems		$\log k_2$
	$\log \beta_{110}$	$\log \beta_{120}$	
Hmpp	6.8 ± 0.1	12.1 ± 0.1	5.3 ± 0.1
Hetpp	6.81 ± 0.06	11.66 ± 0.06	4.85 ± 0.08
Hdmpp	7.02 ± 0.04	12.15 ± 0.05	5.13 ± 0.06
Hempp	6.5 ± 0.1	11.3 ± 0.1	4.8 ± 0.1
Hmepp	6.5 ± 0.2	11.4 ± 0.1	4.8 ± 0.2
Hdepp	6.19 ± 0.08	10.72 ± 0.07	4.5 ± 0.1

The values follow the Irving–Williams series ($\text{Co}^{2+} < \text{Ni}^{2+} < \text{Cu}^{2+} > \text{Zn}^{2+}$) thus providing additional independent experimental evidence for similar coordination geometry for all the complexes in solution. The values of β_{110} and β_{120} for zinc(II) are ca. 10 times bigger than those of nickel(II) and ca. 10^6 times bigger for copper(II).^[30]

The analysis of the distribution diagrams presented in Figure 5 for one of the cobalt(II) systems shows that the beginning of complex formation is observed for pH values above 4 and the figure shows their predominance above 6 in 1:1 and 1:2 ratios. For a 1:1 metal–ligand ratio the ML species is present in a percentage which is almost double that of ML_2 . On the other hand, for a 1:2 metal–ligand ratio, the predominant complex is ML_2 , with a maximum formation of ca. 100% above pH 9, as expected from the values obtained for the formation constants.

Because of the closeness of the stability constant values the diagrams for the nickel(II) systems (Figure 6) are very similar to those of cobalt(II) systems. The most significant differences concern the relative amount of the ML and ML_2

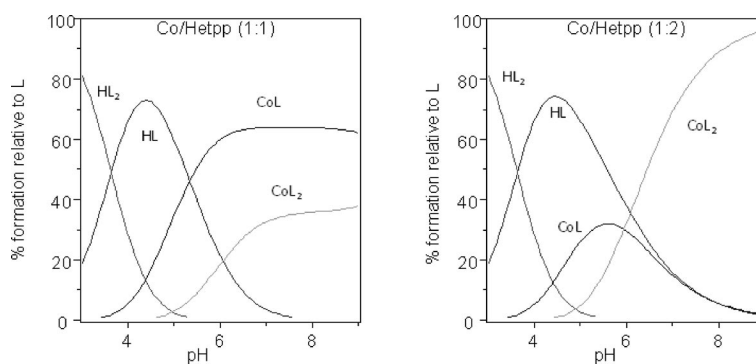


Figure 5. Distribution diagram for the Co^{2+} /Hetpp system with 1:1 and 1:2 metal–ligand molar ratios and a metal concentration of 2 mM (at 298 K and $I = 0.1$ M in NaCl).

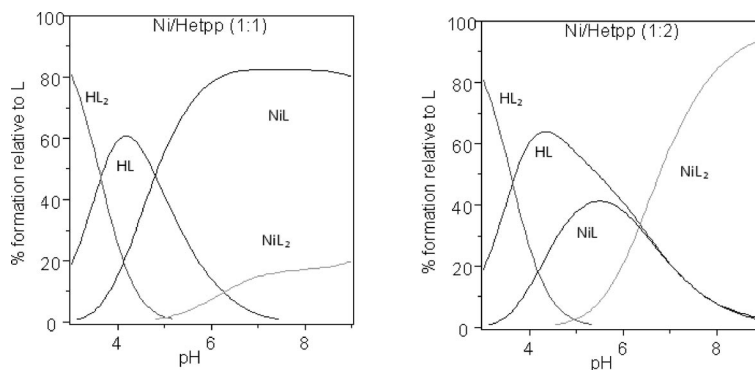


Figure 6. Distribution diagram for the Ni^{2+} /Hetpp system with 1:1 and 1:2 metal–ligand molar ratios and a metal concentration of 2 mM (at 298 K and $I = 0.1$ M in NaCl).

species. For a 1:1 ratio, the percentage of ML formation is approximately 4 times higher than that of ML_2 . For a 1:2 metal–ligand ratio, the predominant complex is ML_2 , with a maximum formation of ca. 100% above pH 8, as expected from the values obtained for the formation constants.

In order to make a comparison of the distribution of species of a particular ligand in the presence of the same amount of Co^{2+} and Ni^{2+} with the biologically relevant M^{II} metal ions Cu^{2+} and Zn^{2+} we plotted Figure 7 in which the curves of the two relevant metal ion species are shown as a function of pH. The figure clearly illustrates the different affinities towards the diverse metal ions and the predominance of the CuL_2 species over all others from pH = 4.5. It is thus demonstrated that these ligands cannot be used orally in the treatment of poisoning with Co^{II} and Ni^{II} ions unless their levels are high enough to avoid unwanted elimination of Fe^{III} , Cu^{II} and Zn^{II} since the latter ions form complexes with higher stability constants. However, since it is possible to vary the substituents on the ligands and to immobilize them in certain matrices, for example sepharose,^[31] they might find application in smart materials. The possibility of capturing nickel(II) or cobalt(II) particles in industrial environments seems worthy of further exploration.

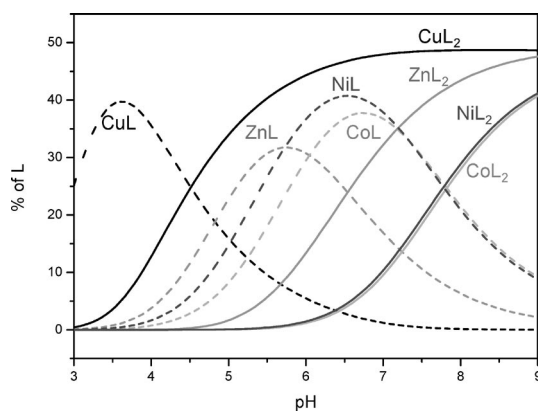


Figure 7. Distribution of species formed by Ni^{II} , Co^{II} , Zn^{II} and Cu^{II} in the presence of the ligand Hdmpp.

Experimental Section

Reagents and Solutions: All reagents were obtained from commercial suppliers as analytical-grade materials and used as received. 3-Hydroxy-2-methyl-4-pyrone (maltol, $\text{C}_6\text{H}_6\text{O}_3$), 2-ethyl-3-hydroxy-4-pyrone (ethylmaltol, $\text{C}_7\text{H}_8\text{O}_3$), 3-hydroxy-1-dimethyl-4-pyridinone (Hdmpp, $\text{C}_7\text{H}_9\text{NO}_2$) were purchased from Sigma–Aldrich, and 0.1 M HCl (Tritisol 9973, Merck), EDTA (Tritisol 9992, Merck), cobalt(II) nitrate [$\text{Co}(\text{NO}_3)_2$], nickel(II) nitrate [$\text{Ni}(\text{NO}_3)_2$], sodium hydroxide (NaOH), sodium chloride (NaCl), methylamine (CH_3NH_2) and ethylamine ($\text{C}_2\text{H}_5\text{NH}_2$) as aqueous solutions (40 or 70%, respectively), were from Merck. Ammonia (NH_3) was obtained from Pronalab. Aqueous solutions were prepared with doubly de-ionized water (conductivity less than $0.1 \mu\text{S cm}^{-1}$).

Synthesis of Ligands: In the present work ligands were prepared using two variants of the direct method. Variant A^[18,19] refers to the direct reaction of the pyrone with the appropriate amine and in variant B^[32] a pH adjustment for the protection of the hydroxide group of the ring is used.

Variant A. Hmpp, Hempp and Hetpp Ligands: Hmpp: an aqueous solution of maltol (119 mmol) was prepared and a large excess of ammonia (225 cm^3) was added; Hempp: an aqueous solution of ethylmaltol (107 mmol) was prepared and an excess of methylamine (67 cm^3) was added; Hetpp: an aqueous solution of ethylmaltol (107 mmol) was prepared and a large excess of ammonia (225 cm^3) was added.

The reaction mixtures were refluxed for 10 h, the amine and solvent surplus removed under reduced pressure and the mixtures allowed to cool to room temperature overnight. The solid products obtained were recrystallized from a mixture of 50% water/methanol in the presence of activated charcoal. The charcoal was filtered off and the volume reduced under pressure. The final products were dried in a desiccator over phosphorus pentoxide. The average yield was found to be 55%.

Variant B. Hmepp, Hdepp and Hempp Ligands: Hmepp: an aqueous solution of maltol (119 mmol) was prepared and ethylamine at 70% (100 cm^3) was added; Hdepp: an aqueous solution of ethylmaltol (214 mmol) was prepared and ethylamine at 70% (100 cm^3) was added; Hempp: an aqueous solution of ethylmaltol (107 mmol) was prepared and methylamine (54 cm^3) was added.

The reaction mixtures were cooled in an ice bath and the pH was adjusted to 9.8 with concentrated HCl and the solutions refluxed for 24 h. The resulting products were extracted with dichloromethane (CH_2Cl_2) and mechanically stirred for 6 h between each extrac-

tion. The solvent was evaporated and the crystals that were formed washed with cold acetone and dried in a desiccator over phosphorus pentoxide. The average yield was found to be 68%.

Synthesis of the Co²⁺ and Ni²⁺ Complexes: The appropriate pyridinone (22 mmol) was dissolved in water and sodium hydroxide (NaOH) (20 mmol) was added. The solution was stirred for 10 min followed by addition of the salt [cobalt(II) or nickel(II) nitrates]. Formation of the complexes begins after reagent mixing and the solution is left under agitation overnight to grant maximum yield. The solid obtained was filtered, washed with the minimum amount of cold water, transferred to a desiccator containing phosphorus pentoxide and after 2 d dried under vacuum for a further 72 h. The water content found in the complexes was quantified by the Karl Fischer method.^[33] The cobalt(II) complexes were isolated in the solid state as pale pink powders and the nickel(II) complexes as green powders.

Physical Measurements: Elemental analyses (C, H, N, Ni/Co) were obtained at Laboratório de Análises do IST, Universidade Técnica de Lisboa and at the Micro Analytical Laboratory Chemistry Department, University of Manchester. Mass spectra (EI and FAB) were obtained at “Unidade de Espectrometria de Massa da Universidade de Santiago de Compostela”, Santiago de Compostela. The water content of the complexes was determined by the Karl Fischer method with a Metrohm KF 737 coulometer. ¹H NMR spectra were obtained with a Bruker AC300 spectrometer at Departamento de Química, Universidade de Aveiro, in deuterated DMSO $\{[(D_6)CH_3]_2SO\}$ with 1% (v/v) TMS. FTIR spectra were obtained with a Mattson 5000 FTIR from 400–4000 cm⁻¹, using KBr for sample preparation. Electronic spectra were recorded with a UNICAM-UV 300 spectrophotometer equipped with a constant-temperature cell holder (25.0 ± 0.1 °C). Spectra of 3 mm solutions of the complexes in DMSO and methanol were recorded in the range 200–1100 nm.

Analytical and Spectroscopic Data of Ligands

3-Hydroxy-2-methyl-4-pyridinone (Hmpp): C₆H₇NO₂ (125.13): calcd. C 57.59, H 5.64, N 11.19; found C 57.50, H 5.68, N 11.20. MS: m/z = 125.2 [M]⁺. ¹H NMR ([D₆]DMSO, 300 Hz, 297 K): δ = 2.169 (s, 3 H, CH₃), 6.067–6.101 [d, 1 H, 5-H], 7.380–7.567 [d, 1 H, 6-H], 11.4 (s, 1 H, NH) ppm. IR (KBr): $\tilde{\nu}$ = 3270 (ν_{OH}), 1643, 1503 (ν_{C=O}), 1538, 1499 (ν_{C=C}), 1299 (ν_{C-O}) cm⁻¹. UV/Vis (DMSO): λ_{max} (ϵ , dm³ mol⁻¹ cm⁻¹) = 283, 927 nm.

2-Ethyl-3-hydroxy-1-methyl-4-pyridinone (Hempp): C₈H₁₁NO₂ (153.18): calcd. C 62.73, H 7.24, N 9.14; found C 62.74, H 7.34, N 9.12. MS: m/z = 153.4 [M]⁺. ¹H NMR ([D₆]DMSO, 300 Hz, 297 K): δ = 1.071–1.176 (t, 3 H, CH₃), 2.641–2.754 (q, 2 H, CH₂), 3.786 (s, 3 H, NCH₃), 6.099–6.062 [d, 1 H, 5-H], 7.509–7.546 [d, 1 H, 6-H] ppm. IR (KBr): $\tilde{\nu}$ = 3200 (ν_{OH}), 1625, 1570 (ν_{C=O}), 1530, 1460 (ν_{C=C}), 1238 (ν_{C-O}) cm⁻¹. UV/Vis (DMSO): λ_{max} (ϵ , dm³ mol⁻¹ cm⁻¹) = 288, 1057 nm.

2-Ethyl-3-hydroxy-2-methyl-4-pyridinone (Hetpp): C₇H₉NO₂ (139.16): calcd. C 60.42, H 6.52, N 10.07; found C 60.40, H 6.53, N 10.05. MS: m/z = 140.0 [M]⁺. ¹H NMR ([D₆]DMSO, 300 Hz, 297 K): δ = 1.100–1.176 (t, 3 H, CH₃), 2.575–2.691 (q, 2 H, CH₂), 6.072–6.106 [d, 1 H, 5-H], 7.416–7.432 [d, 1 H, 6-H] ppm. IR (KBr): $\tilde{\nu}$ = 3255 (ν_{OH}), 1626, 1543 (ν_{C=O}), 1510, 1435 (ν_{C=C}), 1218 (ν_{C-O}) cm⁻¹. UV/Vis (DMSO): λ_{max} (ϵ , dm³ mol⁻¹ cm⁻¹) = 278, 917 nm.

1-Ethyl-3-hydroxy-2-methyl-4-pyridinone (Hmepp): C₈H₁₁NO₂ (153.18): calcd. C 62.73, H 7.24, N 9.14; found C 62.71, H 7.24, N 9.11. MS: m/z = 153.5 [M]⁺. ¹H NMR ([D₆]DMSO, 300 Hz, 297 K): δ = 1.222–1.273 (t, 3 H, CH₃), 3.922–3.994 (q, 2 H, NCH₂),

6.105–6.129 [d, 1 H, 5-H], 7.570–7.592 [d, 1 H, 6-H] ppm. IR (KBr): $\tilde{\nu}$ = 3202 (ν_{OH}), 1620, 1500 (ν_{C=O}), 1530, 1465 (ν_{C=C}), 1242 (ν_{C-O}) cm⁻¹. UV/Vis (DMSO): λ_{max} (ϵ , dm³ mol⁻¹ cm⁻¹) = 286, 1030 nm.

1,2-Diethyl-3-hydroxy-4-pyridinone (Hdepp): C₉H₁₃NO₂ (167.21): calcd. C 64.65, H 7.84, N 8.38; found C 64.28, H 7.93, N 8.26. MS: m/z = 138/167 [M]⁺. ¹H NMR ([D₆]DMSO, 300 Hz, 297 K): δ = 1.100–1.176 (t, 3 H, CH₃), 1.255–1.303 (t, 3 H, NCH₂CH₃), 2.830–2.707 (q, 2 H, CH₂), 4.002–3.931 (q, 2 H, NCH₂), 6.122–6.146 [d, 1 H, 5-H], 7.571–7.595 [d, 1 H, 6-H] ppm. IR (KBr): $\tilde{\nu}$ = 3250 (ν_{OH}), 1598, 1571 (ν_{C=O}), 1515, 1455 (ν_{C=C}), 1250 (ν_{C-O}) cm⁻¹. UV/Vis (DMSO): λ_{max} (ϵ , dm³ mol⁻¹ cm⁻¹) = 298, 953 nm.

Analytical and Spectroscopic Data of Complexes

Bis(3-hydroxy-2-methyl-4-pyridinonate)nickel(II), Ni(mpp)₂: C₁₂H₁₂N₂NiO₄·5H₂O (397.01): calcd. C 40.91, H 4.83, N 7.96, Ni 16.68; found C 40.71, H 4.93, N 8.05, Ni 16.01. MS: m/z = 307 [M]⁺. IR (KBr): $\tilde{\nu}$ = 1655–1590 (ν_{C=O}), 1546–1420 (ν_{C=C}), 1201 (1082) (ν_{C-O}), 485 (M–O) cm⁻¹. UV/Vis (DMSO): λ_{max} (ϵ , dm³ mol⁻¹ cm⁻¹) = 741 (8) nm.

Bis(3-hydroxy-1,2-dimethyl-4-pyridinonate)nickel(II), Ni(dmpp)₂: C₁₄H₁₆N₂NiO₄·5.5H₂O (434.07): calcd. C 38.74, H 6.23, Ni 6.46, Ni 13.53; found C 39.08, H 6.39, Ni 13.70. MS: m/z = 334 [M]⁺, 335 [M + H]⁺, 336 [M + 2H]⁺, 357 [M + Na]⁺, 358 [M + Na + H]⁺. IR (KBr): $\tilde{\nu}$ = 1655–1590 (ν_{C=O}), 1546–1420 (ν_{C=C}), 1201 (1082) (ν_{C-O}) cm⁻¹. UV/Vis (DMSO): λ_{max} (ϵ , dm³ mol⁻¹ cm⁻¹) = 740 (8) nm.

Bis(1-ethyl-3-hydroxy-2-methyl-4-pyridinonate)nickel(II), Ni(mepp)₂: C₁₆H₂₀N₂NiO₄·2.5H₂O (408.08): calcd. C 47.05, H 6.13, Ni 6.86, Ni 14.38; found C 46.99, H 6.25, Ni 6.95, Ni 14.00. MS: m/z = 363 [M]⁺, 364 [M + H]⁺, 365 [M + 2H]⁺, 386 [M + Na]⁺, 387 [M + Na + H]⁺. IR (KBr): $\tilde{\nu}$ = 1657–1615 (ν_{C=O}), 1563–1430 (ν_{C=C}), 1204 (1109) (ν_{C-O}), 479 (M–O) cm⁻¹. UV/Vis (DMSO): λ_{max} (ϵ , dm³ mol⁻¹ cm⁻¹) = 739 (9) nm.

Bis(2-ethyl-3-hydroxy-4-pyridinonate)nickel(II), Ni(etpp)₂: C₁₄H₁₆N₂NiO₄·3H₂O (389.03): calcd. C 43.22, H 5.66, Ni 7.20, Ni 15.10; found C 43.58, H 5.81, Ni 7.27, Ni 15.00. MS: m/z = 335 [M]⁺. IR (KBr): $\tilde{\nu}$ = 1572 (ν_{C=O}), 1576 (ν_{C=C}), 1290 (1089) (ν_{C-O}), 454 (M–O) cm⁻¹. UV/Vis (DMSO): λ_{max} (ϵ , dm³ mol⁻¹ cm⁻¹) = 732 (4) nm.

Bis(2-ethyl-3-hydroxy-1-methyl-4-pyridinonate)nickel(II), Ni(empp)₂: C₁₆H₂₀N₂NiO₄·3H₂O (417.08): calcd. C 46.04, H 6.23, Ni 6.71, Ni 14.07; found C 46.48, H 6.54, Ni 6.85, Ni 14.00. MS: m/z = 363 [M]⁺. IR (KBr): $\tilde{\nu}$ = 1627–1582 (ν_{C=O}), 1436 (ν_{C=C}), 1255 (1070) (ν_{C-O}), 458 (M–O) cm⁻¹. UV/Vis (DMSO): λ_{max} (ϵ , dm³ mol⁻¹ cm⁻¹) = 735 (8) nm.

Bis(1,2-diethyl-3-hydroxy-4-pyridinonate)nickel(II), Ni(depp)₂: C₁₈H₂₄N₂NiO₄·4H₂O (463.15): calcd. C 46.68, H 6.92, Ni 6.05, Ni 12.69; found C 46.08, H 6.80, Ni 6.20, Ni 13.00. MS: m/z = 392 [M]⁺. IR (KBr): $\tilde{\nu}$ = 1640–1570 (ν_{C=O}), 1510–1495 (ν_{C=C}), 1230 (1082) (ν_{C-O}), 467 (M–O) cm⁻¹. UV/Vis (DMSO): λ_{max} (ϵ , dm³ mol⁻¹ cm⁻¹) = 757 (8) nm.

Bis(3-hydroxy-2-methyl-4-pyridinonate)cobalt(II), Co(mpp)₂: C₁₂H₁₂CoN₂O₄·4H₂O (379.23): calcd. C 38.00, H 5.27, Ni 7.39, Co 15.55; found C 37.86, H 5.34, Ni 7.42, Co 15.80. MS: m/z = 307 [M]⁺, 308 [M + H]⁺. IR (KBr): $\tilde{\nu}$ = 1590–1570 (ν_{C=O}), 1470 (ν_{C=C}), 1251 (1082) (ν_{C-O}), 590 (M–O) cm⁻¹. UV/Vis (DMSO): λ_{max} (ϵ , dm³ mol⁻¹ cm⁻¹) = 529 (34) nm.

Bis(3-hydroxy-1,2-dimethyl-4-pyridinonate)cobalt(II), Co(dmpp)₂: C₁₄H₁₆CoN₂O₄·5H₂O (425.30): calcd. C 39.51, H 6.11, Ni 6.58, Co 13.86; found C 39.53, H 6.40, Ni 6.61, Co 14.00. MS: m/z = 335

$[M]^+$. IR (KBr): $\tilde{\nu}$ = 1662–1586 ($\nu_{C=O}$), 1561–1419 ($\nu_{C=C}$), 1200 (1080) (ν_{C-O}), 547 (M–O) cm^{-1} . UV/Vis (DMSO): λ_{max} (ϵ , $\text{dm}^3 \text{mol}^{-1} \text{cm}^{-1}$) = 553 (32) nm.

Bis(1-ethyl-3-hydroxy-2-methyl-4-pyridinonate)cobalt(II), Co(mepp)₂: $\text{C}_{16}\text{H}_{20}\text{CoN}_2\text{O}_4 \cdot 2\text{H}_2\text{O}$ (399.31): calcd. C 48.12, H 6.02, N 7.02, Co 14.77; found C 48.02, H 6.21, N 6.94, Co 15.00. MS: m/z = 363 $[M]^+$. IR (KBr): $\tilde{\nu}$ = 1670–1582 ($\nu_{C=O}$), 1520 ($\nu_{C=C}$), 1190 (1089) (ν_{C-O}), 552 (M–O) cm^{-1} . UV/Vis (DMSO): λ_{max} (ϵ , $\text{dm}^3 \text{mol}^{-1} \text{cm}^{-1}$) = 552 (36) nm.

Bis(2-ethyl-3-hydroxy-4-pyridinonate)cobalt(II), Co(etpp)₂: $\text{C}_{14}\text{H}_{16}\text{CoN}_2\text{O}_4 \cdot 2\text{H}_2\text{O}$ (343.20): calcd. C 41.99, H 4.67, N 8.16, Co 17.18; found C 41.06, H 4.81, N 7.98, Co 17.00. MS: m/z = 307 $[M]^+$. IR (KBr): $\tilde{\nu}$ = 1578 ($\nu_{C=O}$), 1478 ($\nu_{C=C}$), 1286 (1095) (ν_{C-O}), 584 (M–O) cm^{-1} . UV/Vis (DMSO): λ_{max} (ϵ , $\text{dm}^3 \text{mol}^{-1} \text{cm}^{-1}$) = 551 (38) nm.

Bis(2-ethyl-3-hydroxy-1-methyl-4-pyridinonate)cobalt(II), Co(emp)₂: $\text{C}_{16}\text{H}_{20}\text{CoN}_2\text{O}_4 \cdot 3\text{H}_2\text{O}$ (390.30): calcd. C 46.05, H 6.24, N 6.72, Co 14.13; found C 46.67, H 6.44, N 6.74, Co 14.00. MS: m/z = 363 $[M]^+$, 364 $[M + H]^+$, 386 $[M + Na]^+$. IR (KBr): $\tilde{\nu}$ = 1579 ($\nu_{C=O}$), 1530–1441 ($\nu_{C=C}$), 1198 (1078) (ν_{C-O}), 589 (M–O) cm^{-1} . UV/Vis (DMSO): λ_{max} (ϵ , $\text{dm}^3 \text{mol}^{-1} \text{cm}^{-1}$) = 553 (31) nm.

Bis(1,2-diethyl-3-hydroxy-4-pyridinonate)cobalt(II), Co(depp)₂: $\text{C}_{18}\text{H}_{24}\text{CoN}_2\text{O}_4 \cdot 2.5\text{H}_2\text{O}$ (436.37): calcd. C 49.55, H 6.65, N 6.42, Co 13.52; found C 49.94, H 6.56, N 6.39, Co 13.80. MS: m/z = 392 $[M + H]^+$. IR (KBr): $\tilde{\nu}$ = 1680–1590 ($\nu_{C=O}$), 1560–1440 ($\nu_{C=C}$), 1275 (1062) (ν_{C-O}), 591 (M–O) cm^{-1} . UV/Vis (DMSO): λ_{max} (ϵ , $\text{dm}^3 \text{mol}^{-1} \text{cm}^{-1}$) = 571 (34) nm.

Dissociation and Stability Constant Determination: All solutions were prepared with double de-ionized water (conductivity less than 0.1 $\mu\text{S cm}^{-1}$). Solutions of NaOH were prepared in de-ionized water previously purged with argon while boiling to reduce carbonate impurity. Potentiometric measurements were performed with a Crison 2002 decimillivoltmeter and a Crison 2031 automatic burette controlled by an IBM 425SX computer. The electrode assembly consisted of a Russell 900029/4 double junction Ag/AgCl reference electrode and a Russell 18026/02 glass electrode as indicator. All titrations were carried out in a thermostat-controlled double-walled glass cell at $(25.0 \pm 0.1)^\circ\text{C}$ under argon atmosphere, homogeneity of the solutions was ensured by agitation using a Crison 2038 magnetic stirrer and ionic strength was adjusted to 0.10 M with NaCl. System calibration was performed by the Gran method^[34] in terms of hydrogen ion concentration by titrating solutions of strong acid with strong base. Before each run a calibration was performed to check the electrode behaviour. Stock solutions of 3-hydroxy-4-pyridinones (1.0×10^{-2} M) were prepared in water ($I = 0.10$ M NaCl). Aqueous cobalt(II) and nickel(II) nitrate solutions (1.0×10^{-2} to 2.0×10^{-2} M) were standardized with EDTA. For the determination of the acid dissociation constants of the 3,4-HPO ligands an aqueous solution (1 mM) of the deprotonated ligand was titrated with NaOH (ca. 0.03 M, $I = 0.1$ M NaCl, $25.0 \pm 0.1^\circ\text{C}$) under an argon atmosphere. The determination of the stability constants of the binary complexes was performed by titration of $\text{H}^+(\text{aq.})$ (1.0 – 2.0 mM, $I = 0.1$ M NaCl, 25.0°C) in the presence of $\text{Co}(\text{NO}_3)_2$ or $\text{Ni}(\text{NO}_3)_2$ (2.0 mM) and the 3-hydroxy-4-pyridinone ligands (2.0 – 4.0 mM) with NaOH (ca. 3.0×10^{-2} M) under an argon atmosphere.

The stability constants were determined from data of experiments in which 1:1, 1:2 and 1:3 metal–ligand ratios were used, and each titration was performed 5 times to ensure the reproducibility of the data.

The global equilibrium constants defined by Equations (6) and (7) were refined by least-squares calculation using the computer pro-

gram Hyperquad^[22] taking into account the presence of the hydroxide species of cobalt and nickel and the auto-protolysis of water. The errors associated to the β_{pqr} values were determined using the Albert & Sergeant theory.^[35]



$$\beta_{pqr} = [M_pL_qH_r]^{2p-q+r}/[M]^p[L]^q[H]^r \quad (7)$$

M is the metal, L the 3,4-HPO in its anionic form, H^+ the proton and p , q , r the stoichiometric coefficients)

Computational Methods: DFT has been proved to be extremely useful in treating the electronic structures of molecules containing transition metals. In this work we used DFT to fully optimize the geometries of a series of nickel(II) and cobalt(II) complexes in the gas phase without any symmetry constraint. Becke's three-parameter exchange-correlation hybrid functional (B3LYP) with nonlocal correlation corrections, provided by Lee, Yang and Parr was used.^[36–40] The double-zeta Pople basis set 6-31G(d,p) was employed, which ensures a superior electronic description by adding polarization functions of the p, d and, especially, f-type for all the hydrogen, non-hydrogen and metal atoms, respectively. Since all the complexes contain unpaired electrons, unrestricted open-shell calculations were carried out using the Gaussian03 quantum mechanical package.^[40] Graphical representations of all the optimized structures were produced with the MOLEKEL 4.3 package.^[41]

Supporting Information (see also the footnote on the first page of this article): Mass spectroscopic data for the cobalt(II) and nickel(II) complexes are provided in Table S1.

Acknowledgments

Financial support by the Fundação para a Ciência e Tecnologia (FCT) is gratefully acknowledged.

- [1] J. Burgess, M. Rangel, *Adv. Inorg. Chem.* **2008**, *60*, 167–243.
- [2] S. Fernandes, A. Nunes, A. R. Gomes, B. Castro, R. C. Hider, M. Rangel, R. Appelberg, M. S. Gomes, *Microbes Infection* **2010**, 287–294.
- [3] D. E. Green, M. L. Bowen, L. E. Scott, T. Storr, M. Merkel, K. Böhmerle, K. H. Thompson, B. O. Patrick, H. J. Schugar, C. Orvig, *Dalton Trans.* **2010**, 39, 1604–1615.
- [4] R. Grazina, L. Gano, J. Šebestík, M. A. Santos, *J. Inorg. Biochem.* **2009**, *103*, 262–273.
- [5] T. Zhou, X. Kong, D. Y. Liu, Z. D. Liu, R. C. Hider, *Biomacromolecules* **2008**, *9*, 1372–1380.
- [6] S. Fakih, M. Podinovskaia, X. Kong, H. L. Collins, U. E. Schaible, R. C. Hider, *J. Med. Chem.* **2008**, *51*, 4539–4552.
- [7] J. Burgess, B. Castro, C. Oliveira, M. Rangel, W. Schlindwein, *Polyhedron* **1997**, *16*, 789–794.
- [8] P. S. Dobbin, R. C. Hider, A. D. Hall, P. D. Taylor, P. Sarpong, J. B. Porter, G. Xiao, D. van der Helm, *J. Med. Chem.* **1993**, *36*, 2448–2458.
- [9] R. C. Scarrow, P. E. Riley, K. Abu-Dari, D. L. White, K. N. Raymond, *Inorg. Chem.* **1985**, *24*, 954–967.
- [10] M. Santos, M. Gil, L. Gano, S. Chaves, *J. Biol. Inorg. Chem.* **2005**, *10*, 564–580.
- [11] R. C. Hider, T. Zhou, *Ann. N. Y. Acad. Sci.* **2005**, *1054*, 141–154.
- [12] E. J. Neufeld, *Blood* **2006**, *107*, 3436–3441.
- [13] K. H. Thompson, C. Orvig, *Dalton Trans.* **2006**, 761–764.
- [14] O. Andersen, *Chem. Rev.* **1999**, *99*, 2683–2710.
- [15] N. Gault, C. Sandre, J.-L. Poncy, C. Moulin, J.-L. Lefaix, C. Bresson, *Toxicol. Vitro* **2010**, *24*, 92–98.

- [16] K. S. Kasprzak, F. W. Sunderman Jr., K. Salnikowa, *Mutat. Res.* **2003**, 533, 67–97.
- [17] S. M. Cohen, *Curr. Opin. Chem. Biol.* **2007**, 11, 115–120.
- [18] W. O. Nelson, T. B. Karpishin, S. J. Rettig, C. Orvig, *Can. J. Chem.* **1988**, 66, 123–131.
- [19] Z. R. Zhang, S. T. Rettig, C. Orvig, *Can. J. Chem.* **1992**, 70, 763–770.
- [20] C. Gérard, *Bull. Soc. Chim. Fr.* **1979**, 11, I451–I456.
- [21] S. I. Ahmed, J. Burgess, J. Fawcett, S. A. Parsons, D. R. Russell, S. H. Laurie, *Polyhedron* **2000**, 19, 129–135.
- [22] P. Gans, A. Sabatini, A. Vacca, *Talanta* **1996**, 43, 1739–1753.
- [23] P. Buglyó, T. Kiss, E. Kiss, D. Sanna, E. Garribba, G. Micera, *J. Chem. Soc., Dalton Trans.* **2002**, 2275–2282.
- [24] D. J. Clevette, D. M. Lyster, W. O. Nelson, T. Rihela, G. A. Webb, C. Orvig, *Inorg. Chem.* **1990**, 29, 667–672.
- [25] M. A. Santos, R. Grazina, A. Q. Neto, G. Cantino, L. Gano, L. Patricio, *J. Inorg. Biochem.* **2000**, 78, 303–311.
- [26] M. Rangel, M. J. Amorim, E. Garriba, G. Micera, E. Lodyga-Chruscinska, *Inorg. Chem.* **2006**, 45, 8086–8097.
- [27] P. Buglyó, I. Fábán, E. Kiss, T. Kiss, D. Sanna, E. Garribba, G. Micera, *Inorg. Chim. Acta* **2000**, 306, 174–183.
- [28] D. M. Doble, B. ÓSullivan, C. Siering, J. D. Xu, V. C. Pierre, K. N. Raymond, *Inorg. Chem.* **2003**, 42, 4930–4937.
- [29] Academic software, *IUPAC stability constants data base*, SC data base, **2009**.
- [30] M. Rangel, P. Gameiro, *unpublished results*.
- [31] M. A. Esteves, A. Cachudo, S. Chaves, M. A. Santos, *Eur. J. Inorg. Chem.* **2005**, 597–605.
- [32] W. O. Nelson, S. J. Rettig, C. Orvig, *Inorg. Chem.* **1989**, 28, 3153–3157.
- [33] K. Fischer, *Angew. Chem.* **1935**, 48, 394–396.
- [34] G. Gran, *Analyst* **1952**, 77, 661–671.
- [35] A. Albert, E. P. Sergeant, *The Determination of Ionization Constants*, 2nd ed., Chapman & Hall, London, **1971**.
- [36] A. D. Becke, *J. Chem. Phys.* **1993**, 98, 5648–5652.
- [37] A. D. Becke, *Phys. Rev. A* **1988**, 38, 3098–3100.
- [38] C. Lee, W. Yang, R. G. Parr, *Phys. Rev. B* **1988**, 37, 785–789.
- [39] P. J. Stevens, F. J. Devlin, C. F. Chabalowski, M. J. Frisch, *J. Chem. Phys.* **1994**, 98, 11623–11627.
- [40] M. J. Frisch, G. W. Trucks, H. B. Schlegel, G. E. Scuseria, M. A. Robb, J. R. Cheeseman, J. A. Montgomery Jr., T. Vreven, K. N. Kudin, J. C. Burant, J. M. Millam, S. S. Iyengar, J. Tomasi, V. Barone, B. Mennucci, M. Cossi, G. Scalmani, N. Rega, G. A. Petersson, H. Nakatsuji, M. Hada, M. Ehara, K. Toyota, R. Fukuda, J. Hasegawa, M. Ishida, T. Nakajima, Y. Honda, O. Kitao, H. Nakai, M. Klene, X. Li, J. E. Knox, H. P. Hratchian, J. B. Cross, V. Bakken, C. Adamo, J. Jaramillo, R. Gomperts, R. E. Stratmann, O. Yazyev, A. J. Austin, R. Cammi, C. Pomelli, J. W. Ochterski, P. Y. Ayala, K. Morokuma, G. A. Voth, P. Salvador, J. J. Dannenberg, V. G. Zakrzewski, S. Dapprich, A. D. Daniels, M. C. Strain, O. Farkas, D. K. Malick, A. D. Rabuck, K. Raghavachari, J. B. Foresman, J. V. Ortiz, Q. Cui, A. G. Baboul, S. Clifford, J. Cioslowski, B. B. Stefanov, G. Liu, A. Liashenko, P. Piskorz, I. Komaromi, R. L. Martin, D. J. Fox, T. Keith, M. A. Al-Laham, C. Y. Peng, A. Nanayakkara, M. Challacombe, P. M. W. Gill, B. Johnson, W. Chen, M. W. Wong, C. Gonzalez, J. A. Pople, *Gaussian 03*, rev. C.02, Gaussian Inc., Wallingford, CT, **2004**.
- [41] P. Flükiger, H. P. Lüthi, S. Portmann, J. Weber, *MOLEKEL 4.3*, Molecular Visualization Software, Swiss Center for Scientific Computing, Manno, Switzerland, **2000**.

Received: August 6, 2010

Published Online: November 25, 2010